

Enhanced surface hydrophobicity of poly(lactic acid) by Co^{60} gamma ray irradiation

S. Galindo and F. Ureña-Núñez

*Instituto Nacional de Investigaciones Nucleares,
km 36.5, Carretera México-Toluca, Ocoyoacac, Estado de México, 52750, México,
e-mail: salvador.galindo@inin.gob.mx; fernando.urena@inin.gob.mx*

Received 26 July 2017; accepted 16 August 2017

Contact angle measurements were performed on Co^{60} gamma-ray irradiated poly(lactic acid) (PLA) samples at several doses, using the sessile drop method. It was found that irradiation alters the wettability of PLA. In particular, PLA wetting behavior changes from moderately hydrophilic at low dose (< 100 kGy), to hydrophobic after the samples were exposed above a threshold dose (≈ 200 kGy). At low doses, wettability follows the Wenzel relation but beyond a threshold dose the Cassie-Baxter regime takes place. Scanning electron microscopy (SEM) and atomic force microscopy (AFM) show that surface roughness of the samples increases as the applied dose increases. PLA wettability changes are mainly a consequence of surface modifications as roughness promotes the formation of air pockets under a drop, which reinforces the hydrophobic nature of its surface. Co^{60} gamma ray irradiation can be used to tailor wetting properties of PLA. The method might have also application to produce biphilic PLA. Finally it is very important to remark that reported contact angles values for PLA (by different authors) of untreated samples vary from 60 to 85 degrees. Reasons for this behavior are given in this article.

Keywords: Poly(lactic acid); wettability; gamma-irradiation; surface morphology; Cassie-Baxter; Wenzel.

Se realizaron mediciones de ángulos de contacto en muestras de ácido poli-láctico (PLA) irradiadas con rayos gamma Co^{60} a varias dosis, usando el método de gota sécil. Se encontró que la irradiación altera la humectabilidad del PLA. En particular, el comportamiento de humectación de PLA cambia de moderadamente hidrófilo a dosis bajas (< 100 kGy), a hidrófobo después de que las muestras fueron expuestas por encima de una dosis umbral (≈ 200 kGy). A dosis bajas, la humectabilidad sigue la relación de Wenzel pero más allá de una dosis umbral el régimen de Cassie-Baxter tiene lugar. Microscopía electrónica de barrido (SEM) y microscopía de fuerza atómica (AFM) muestran que la rugosidad superficial de las muestras aumenta a medida que aumenta la dosis aplicada. Los cambios de humectabilidad del PLA son principalmente una consecuencia de las modificaciones superficiales, ya que la rugosidad promueve la formación de bolsas de aire bajo la gota, lo que refuerza la naturaleza hidrófoba de la superficie. La irradiación con rayos gamma de Co^{60} puede usarse para modificar las propiedades de humectación del PLA. El método podría tener también aplicación para producir PLA bifílico. Finalmente, es muy importante señalar que los valores de ángulos de contacto reportados para PLA (por diferentes autores) de muestras no tratadas varían de 60 a 85 grados. Las razones de este comportamiento se proporcionan en este artículo.

Descriptores: Ácido poliláctico; mojabilidad; irradiación gama; morfología superficial; Cassie-Baxter; Wenzel.

PACS: 68,08.Bc; 61,82.Pv; 68,47.Mn; 68,36.bm

1. Introduction

The last decades of research in polymer science and technology have seen a sharp rise in the attention given to the development of materials produced from renewable resources as an alternative to conventional petroleum-based polymers. One of such materials is poly(lactic acid) (PLA), which is a readily biodegradable thermoplastic with reasonably good optical, physical, mechanical, and barrier properties (Auras *et al.*, 2003). This plastic has generated great interest as one of the most innovative materials being developed for a wide range of applications (Rasal and Hirt, 2009, Ray and Okamoto, 2003, Zhang and Feng, 2006, Gottschalk and Frey, 2006, Zhu *et al.*, 1990, Schugens *et al.*, 1995, Okada 2002), (Tsuji 2016). Moreover, PLA has the advantage that is obtained from agricultural sources, such as corn, starch and sugar cane.

Surface properties of PLA such as charge, conductivity, roughness, porosity, wettability, friction, physical and chemical reactivity and biocompatibility, are important in several applications. Therefore different modification methods have

been developed to tailor PLA surface properties. For example PLA surface wettability can be modified by the use of several techniques such as: plasma treatment (Hergelová, 2015), surface coating (Hendrick and Frey, 2014), or photografting (Rasal and Hirt, 2010).

It is the intention of the present study to report PLA surface wettability changes after being irradiated with Co^{60} gamma rays at several doses. For this purpose, contact angle measurements were used to evaluate the wettability of the untreated and gamma-irradiated PLA samples. We found that the initially slightly hydrophilic PLA (approx. contact angle $\theta \approx 60^\circ$) of non-irradiated samples becomes increasingly hydrophobic with increasing irradiation doses, reaching at high doses, contact angles in the vicinity of 85° .

Given that the observed changes in surface wettability of PLA may be due to either topography effects or to modification of PLA surface chemistry or both, we performed Atomic Force Microscopy (AFM), Scanning Electron Microscopy (SEM) and X-ray Photoelectron Spectroscopy (XPS) studies on the samples to investigate the cause of such wettability changes. The former pair of techniques (AFM and SEM) was

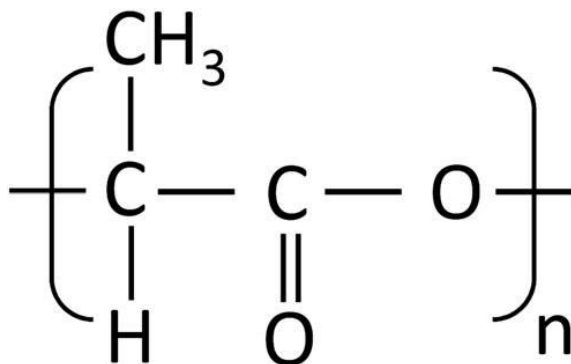


FIGURE 1. Chemical structure of poly(lactic acid).

employed to visualize and compare topographic changes of untreated and irradiated PLA surfaces while possible chemical surface composition changes on the samples, were studied using XPS.

2. Experimental

2.1. Materials

PLA Biopolymer 2003D sheets of high molecular weight were provided by IngeoTM (Ingeo, 2003). Thickness of the sheets was approximately 0.25 mm. The chemical structure PLA is shown in Fig. 1.

2.2. Sample irradiation

Samples were exposed to several ⁶⁰Co gamma radiation doses of: 100, 200, 400, 600, 800, 1000 and 1300 kGy, in air at room temperature. A dose rate of 3.5 kGy/h was applied using a Transelektro irradiator model LGI-01.

2.3. Contact Angle Measurement

A homemade instrument equipped with a CCD camera was used to measure contact angles of water on samples by sessile drop method under constant temperature and humidity condition (25°C, 65% RH). Distilled water was used. The volume of the drop placed with a micropipette on the surface of an examined sample was 3 mm³. The time that elapsed, from the moment the drop was placed to the moment when a close up snapshot was taken, was within the range of 30-60 s for all the measurements. Before contact angle measurements were performed, samples were previously rinsed with ultra-pure water in an ultrasound bath for 15 min, and then dried in an oven at 40°C for 30 min.

The static contact angle of a drop's profile was measured for each photograph using the software package, ImageJ (ImageJ, 2015), with the dropsnake plugin (Stalder *et al.*, 2006). This plugin was employed to define the contour of the drop as a B-spline curve, which was extended by mirror symmetry to determine the interfacial contact points. Twelve measurements were performed for each sample; the lowest and the highest angle values were disregarded and the remaining ten

were used to calculate the arithmetic mean, and standard deviation, the last quantity being of the order of 3 degrees or less.

2.4. XPS Measurements

Chemical composition of the surface samples was determined by X-ray photoelectron spectroscopy (XPS) using a Thermo Scientific, K-Alpha model spectrometer, employing a monochromatic Al K α (1486.6 eV) X-ray source. The diameter of the analysis area was 400 μ m. The base pressure of the analysis chamber was 10⁻⁹ mbar; however, a beam of Ar ions was applied to the samples to reduce electrostatic charges on their surfaces. This action increased the pressure in the chamber up to 10⁻⁷ mbar in which the analyses were performed. The overview survey spectra were taken between 50 and 1300 eV with an energy step of 0.5 eV, while the detailed spectra of the peaks of interest (O 1s and C 1s) were recorded with an energy step of 0.1 eV. The overlapping peaks in detailed spectra were resolved by the peak synthesis method, applying Gaussian peak components after a straight line background subtraction.

2.5. Scanning Electron Microscopy

Surface topography was examined with a JEOL JSM 5900LV scanning electron microscope (SEM). With this SEM, samples can be observed without the need for coating by using the low vacuum capability of the instrument.

2.6. Atomic Force Microscopy (AFM)

AFM measurements were carried out for quantification of the surface area of the samples before and after gamma irradiations. In this way surface area changes of the samples, contributed by alterations in the surface texture, were estimated. The AFM used was a CypherTM S (Asylum Research), operated in AC mode. The images were collected at a fixed scan rate of 1 Hz. The sampling rate was 256 samples/line and the XY Scan Range of 30 μ m.

3. Results

3.1. Wettability

To investigate the effects of gamma-ray irradiation on wettability, static contact angle measurements were carried out. Figure 2 shows the variation of contact angle with different gamma-ray doses. The contact angle value on pristine PLA was measured to be 60.1° (\pm 1.3°), similar to one value already reported in literature (Koo and Jang, 2008). However, it is very important to remark that reported contact angles values for PLA (by different authors) of untreated samples vary from 60 to 85 degrees. Reasons for this behavior will be discussed later in this article.

As shown in Fig. 2 contact angle tendency at the start, is to slightly reduce its value at low applied doses, but after a

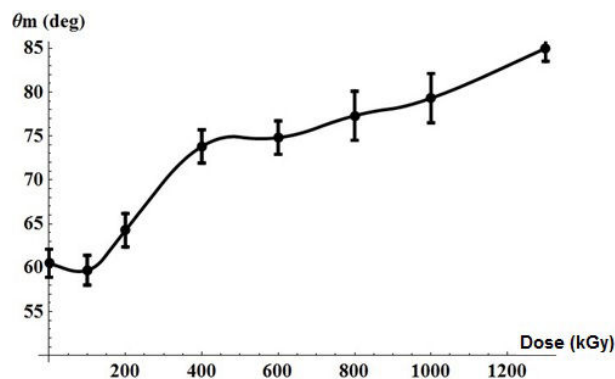


FIGURE 2. Variation of contact angle with different gamma-ray doses.

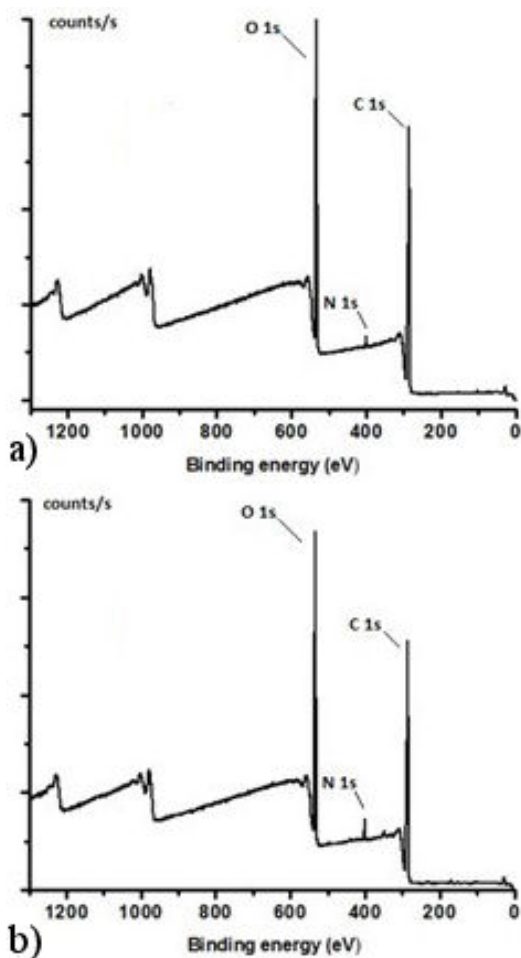


FIGURE 3. XPS survey spectra of a) non-irradiated sample b) irradiated at 1300 kGy dose.

200 kGy dose is applied, contact angle value abruptly grows as the dose escalates, reaching a low incline plateau trend at 400 kGy dose.

3.2. Chemistry changes versus Topography

It is well known that observed changes in the contact angle values may be due to alterations of surface chemistry of the

samples and/or to modifications in surface topography. We shall first consider the question of surface chemistry changes.

3.2.1. Chemical Surface Composition

To quantitatively investigate the issue of chemical alterations on the samples surface, that may lead to changes in its wettability, we carried out an XPS analysis on them. Fig. 3 shows representative XPS survey spectra for two samples, namely the non-irradiated PLA sample (0 kGy), and the sample irradiated at maximum dose (1300 kGy).

The PLA surface atomic composition for both samples is reported in Table I. It can be seen from values in Table I that irradiation treatment caused no major changes in the PLA surface atomic composition as the carbon to oxygen ratio for the irradiated sample remains nearly equal to the theoretical stoichiometric carbon to oxygen ratio of PLA ($C/O = 3/2$). Contaminants of Si and S were also found. Results at other intermediate doses are similar and are not shown. However, a peculiar result of the irradiation treatment is an increase on the surface of PLA of a small amount of nitrogen, already present in the untreated sample. After a 1300 kGy dose was applied, the nitrogen to carbon and to oxygen ratios (N/C or N/O) approximately augmented twice their values for both cases, from those of the untreated sample. We shall comment on this later.

The XPS high resolution C 1s peak decomposition for the non-irradiated sample and the sample irradiated at maximum dose is shown in Fig. 4. Samples showed three well resolved components at 285.0 eV, 287.2 eV and 289.08 eV. The peak at 285.0 eV corresponds to aliphatic carbons (C-C) and hydrocarbons (C-H) present in PLA, while the peaks at 287.0 and 289.1 eV can be attributed to C-O and O-C=O groups respectively.

Table II presents the XPS C 1s relative peak areas, corresponding to the three mentioned carbon-containing bonds. Small changes in the relative peak areas are observed after irradiation treatment. On the one hand C-O area grows after the sample was irradiated, whereas for the other two functional groups, their areas suffer a small percentage decrement. In relation to these area changes, we must consider two points: on the one hand, survey spectra as we have already mentioned, shows a small increment of the nitrogen content on the sur-

TABLE I. Atomic Concentration of surface composition, for non-irradiated and gamma irradiated sample at a maximum dose (1300 kGy) obtained from XPS measurements.

Dose (kGy)	Survey spectrum (Atomic %)				
	C 1s	O 1s	N 1s	Si 2p	S 2p
0	63.64	34.03	1.61	0.72	
1300	63.1	32.03	3.43	0.85	0.59
Nominal stoichiometric	66.67	33.33	0	0	0

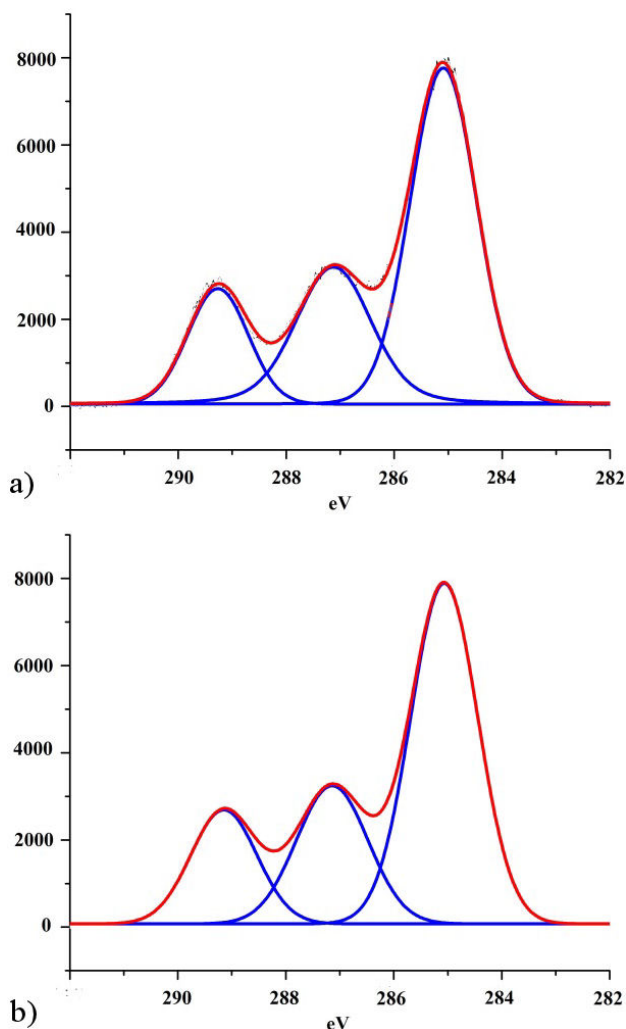


FIGURE 4. High-resolution C 1s peaks of PLA (a) before and (b) after been irradiated at maximum dose (1300 kGy).

TABLE II. C 1s components.

Functional group	Peaks eV	Area (C 1s %)		
		0 kGy	1300 kGy	Δ area (%)
C-C/C-H	285.	55.28	54.26	- 1.02
C-O	287	27.68	29.08	1.4
O-C=O	289.1	17.04	16.65	-0.39

face of the irradiated sample and, on the other hand, the energy difference between C-N (286.2 eV) and C-O (287.2) functional groups is small (Briggs, 1990, Morent, 2008). These two circumstances could mean that, if a small amount of nitrogen is being integrated to the surface of PLA as C-N groups, the incorporation of them will appear as a small overlapped line that might be adding area to the C-O group due to its nearness increasing its area, in detriment of the percentage contributions of the other two groups (C-C/C-H and O-C=O). This could explain small changes noticed in the XPS spectrum.

However, changes in hydrophobicity should not be attributed to nitrogen incorporation. Nitrogen incorporation on PLA surface has been previously reported in literature after PLA samples were exposed to a medium pressure Dielectric Barrier Discharge (DBD) (De Geyter, 2013). In addition, it was also reported that DBD exposure produced a slight increase in hydrophobicity of the material. Nevertheless nitrogen addition to PLA surface is not an obvious cause of PLA hydrophobicity enhancement as the mentioned DBD discharges on PLA noticeably modified its surface chemistry. Specifically, DBD treatment resulted in significant buildup of C-O and O-C=O bonds, and a new C-O-C peak at 286.5 eV emerged in the XPS spectrum. In contrast, the present work shows no major changes in either chemical composition or functional groups modifications on the surface after gamma ray irradiation. So we must consider other reasons to explain the observed hydrophobicity change.

3.2.2. Roughness and Wetting

We will now direct our attention to the dependence between surface roughness and its wetting. In practice it is possible to alter the wetting properties of a substrate by changing the roughness of its surface r defined as the ratio of the real surface area to the apparent surface area. There are two basic models to describe the apparent contact angle of a drop on rough surfaces. One was proposed by Wenzel and is described by the following relation (Wenzel, 1949):

$$\cos \theta_W = r \cos \theta_Y \quad (1)$$

where θ_W is the actual contact angle on a real uneven surface or Wenzel's angle, r is its roughness, and θ_Y is the equilibrium Young contact angle expected on an ideally smooth surface. This model assumes that the liquid penetrates into the nooks and crannies of the substrate. Since r is always greater than 1, this model predicts an enhanced hydrophilicity ($\theta_W < \theta_Y$) for hydrophilic surfaces ($\theta_Y < 90^\circ$), and a higher hydrophobicity ($\theta_W > \theta_Y$) for hydrophobic surfaces ($\theta_Y > 90^\circ$).

The second model was developed by Cassie and Baxter (Cassie and Baxter, 1944). It supposes that the liquid does not

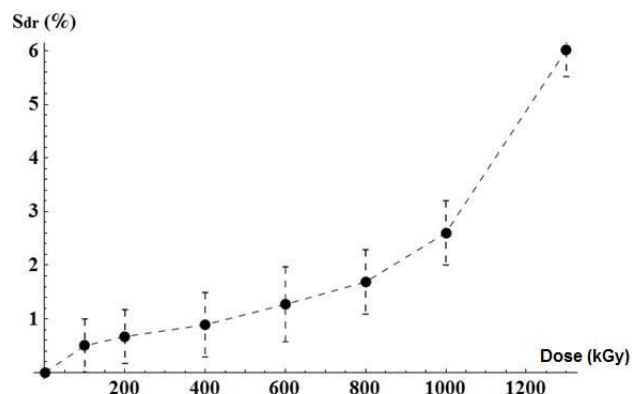


FIGURE 5. Variation of the area factor S_{dr} with irradiation dose.

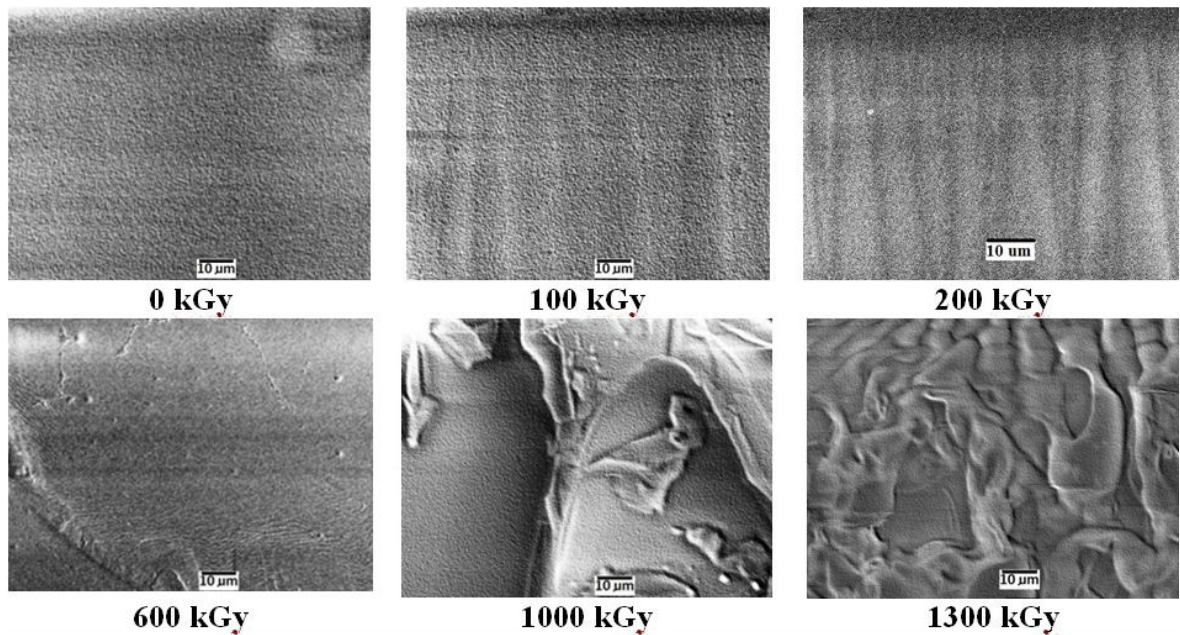


FIGURE 6. SEM images of gamma irradiated areas showing topographic changes.

entirely wet the uneven substrate. This condition can be expressed by the following equation (Marmur, 2003):

$$\cos \theta_{CB} = r_f f \cos \theta_Y + f - 1 \quad (2)$$

where θ_{CB} is the Cassie-Baxter contact angle, f is the fraction of the solid surface in contact with the liquid, and r_f is the surface ratio of the wet area to its nominal area. If the liquid entirely wets the uneven substrate then, $f = 1$ and $r_f \equiv r$, and the Cassie-Baxter equation reduces to the Wenzel equation. Conversely, in case the liquid partially wets the substrate, f is less than 1 and since r_f is always less than 1, then the Cassie-Baxter model predicts that roughening a surface always increases the contact angle even if the surface chemistry is intrinsically hydrophilic.

3.2.3. Surface topography changes in PLA

There are many parameters describing the topography of a surface (Gadelmawla *et al*, 2002, ISO 25178). Atomic Force Microscopy quantifies a set of them. Some are useful for nanoscale related phenomena and others are suitable for larger scale processes. Here, according to the wetting models mentioned above, the parameter that concerns us is the surface area ratio S_{dr} of the samples, defined as specified by the ISO 25178,

$$S_{dr} = \frac{(\text{textured surface area}) - (\text{cross sectional area})}{\text{cross sectional area}} \times 100 \quad (3)$$

In other words, the ratio between interfacial and projected areas S_{dr} provides the additional surface area contributed by texture. This parameter is especially useful as it can be used

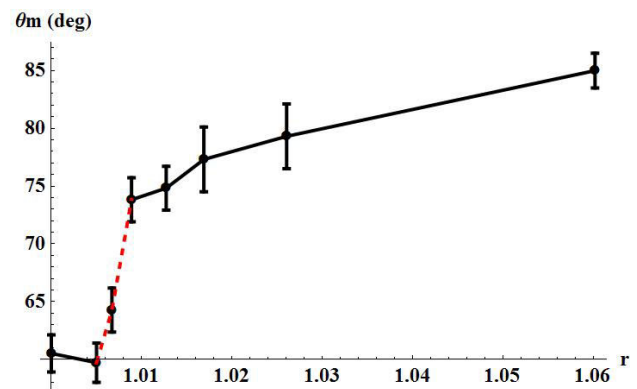


FIGURE 7. Contact angles as function of r the calculated roughness parameter.

to calculate the roughness ratio r , given that by definition it is related to surface roughness r by $S_{dr} = (r - 1)100$.

Using atomic force microscopy measurements we have quantified the surface area ratio S_{dr} of the samples. Figure 5 shows the variation of the area factor S_{dr} with dose.

It is observed that the area factor increases as the dose increases. This happens as PLA surface wrinkles with increasing radiation doses adding area to the sample's surfaces. This fact is readily confirmed by a series of SEM images shown in Fig. 6. It is clearly seen that the PLA substrate goes from a very flat, wrinkle free surface, to a surface full of crevices and pores as radiation dose increases. Figure 7 shows the variation of measured contact angles as function of the calculated roughness parameter r .

The results presented in Fig. 7, reveal that at low dose the hydrophilicity of PLA increases slightly as the PLA surface does in accordance to Wenzel's relation and consequently the

TABLE III. Reported PLA contact angle measurements.

author	angle	Surface topology characterization
This work	$60.1 \pm 1.3^\circ$	AFM
Chaiwong <i>et al.</i> 2010	$60.4 \pm 4.4^\circ$	AFM (rms)
Cai <i>et al.</i> 2002	$69 \pm 3^\circ$	None
Ding <i>et al.</i> 2004	70°	None
De Geyter 2010	75°	None
De Geyter <i>et al.</i> 2013	75°	None
Yu <i>et al.</i> 2006	$76.1 \pm 1.3^\circ$	None
Lück <i>et al.</i> 1998	79.4°	None
Cui <i>et al.</i> 2003	$77.14 \pm 0.53^\circ$	None
Croll, <i>et al.</i> 2004	79°	AFM- rms
Jeon <i>et al.</i> 2013	84.5°	None
Rasal 2009	$82 \pm 0.2^\circ$	None
Khorasani <i>et al.</i> 2008	85°	SEM gold coated samples

contact angle reduces its value. However at a certain threshold roughness (see Fig. 7, around 1.01), the contact angle suddenly jumps to a much higher value. This transition can be interpreted as the sudden formation of air pockets under the drop at that particular roughness (and beyond), due to wrinkles formed on the PLA surface by irradiation treatment. We have already mentioned that surface roughness promotes the formation of air pockets under a drop, which reinforces the hydrophobic nature of the surface. For doses of 400 kGy and above, the Cassie-Baxter relation applies.

3.2.4. Raw PLA contact angle discrepancies

The contact angle of raw PLA has been measured many times by many authors in the past. They have performed these measurements because they have tried to change, by applying different surface treatments, the hydrophilicity of PLA. An inspection of the published literature on the subject reveals that the reported measured contact angle for a PLA untreated sample varies from 60 to 85 degrees (see Table III). The wide discrepancies among reported values seem to be incongruous, as contact angles were supposedly measured on the same material substrate. However one must take into account that surfaces are not ideal, that is to say smooth and chemically homogeneous. We have already given evidence that PLA wettability mainly depends on its surface's roughness.

Unfortunately, the papers that report raw PLA contact angles (see Table III) do not indicate the roughness status of the respective PLA surfaces. At most, in two of the works cited in Table III, the root mean square (rms) of the surface height is given when samples were analyzed by AFM, but not their roughness parameter r . In addition we must point out that another factor altering contact angle measurements is surface impurities. It was shown by De Marco *et al.* that debris on a surface of a polymer strongly affects the contact-angle results leading to apparent spurious measurements. The true contact angle value is revealed after rinsing and drying the samples to measure (De Marco *et al.*, 2010). As already mentioned, our samples were carefully rinsed and subsequently dried before carrying out contact angle measurements.

4. Conclusions

In this work, we have presented an ample and systematic study of surface features of PLA following gamma-ray irradiation at several doses. In summary, Co60 irradiation was found to alter the wettability of PLA. In particular, the PLA wetting behavior changes from moderately hydrophilic (60°) to hydrophobic (85°) after the samples were exposed to a threshold dose (and above). We observed that the changed wettability is mainly a consequence of PLA surface morphology modifications induced at microscales, following irradiation processing. At low doses, wettability follows the Wenzel relation but beyond a threshold dose the Cassie-Baxter regime takes place. The chemistry of the polymeric substrates was not essentially altered after Co⁶⁰ irradiation, as confirmed by spectroscopic analysis.

Gamma-ray irradiation of PLA appears to be a versatile technique for tailoring its wettability. Further, this technique could be applied to produce PLA biphilic surfaces (surfaces which combine hydrophilic and hydrophobic regions), by properly shielding selected regions from gamma rays. It has been recently realized that biphilic surfaces can alter the size and number of droplets on their surfaces at freezing and can delay the time required for a surface to freeze (Van Dyke *et al.*, 2015).

We have pointed out that different contact angle values have been reported for untreated PLA samples. These measurements widely differ from each other. We have further shown that such angle depends strongly on the surface topography of samples. Therefore, we conclude that when reporting contact angle values, the surface morphology must be also included. Unfortunately this is not currently practiced by many researchers, that simply report the angle and occasionally a loosely related surface feature such as its root mean square (rms).

1. R.A. Auras, B. Harte, S. Selke, and R. Hernandez, *Journal of plastic film and sheeting* **19** (2003) 123-135. doi: 10.1177/8756087903039702
2. D. Briggs, in: D. Briggs, M.P. Seah (Eds.), *Practical Surface Analysis Auger and X-ray Photoelectron Spectroscopy*, John Wiley & Sons, Ltd., West Sussex-England, **1** (1990) 437. ISBN 978-0471953401
3. K. Cai, Yao *et al.*, *Biomaterials* **23** (2002) 1603-1611.
4. A.B.D. Cassie and S. Baxter, *Wettability of porous surfaces. Trans. Faraday Soc.* (1944) **40** 546-551. doi: 10.1039/TF9444000546.
5. C. Chaiwong, P. Rachtanapun, P. Wongchaiya, R. Auras, and D. Boonyawan, *Surface and Coatings Technology* **204** (2010) 2933-2939.
6. T.I. Croll, A.J. O'Connor, G.W. Stevens, and J.J. Cooper-White, *Biomacromolecules* **5** (2004) 463-473.
7. Y.L. Cui, A. Di Qi, W.G. Liu, X.H. Wang, H. Wang, D.M. Ma, and K. De Yao, *Biomaterials* **24** (2003) 3859-3868.
8. N. De Geyter, *et al.*, *Surface and Coatings Technology* **204** (2010) 3272-3279. doi.org/10.1016/j.surfcoat.2010.03.037
9. N. De Geyter, *Surface and Coatings Technology* **214** (2013) 69-76. doi:10.1016/j.surfcoat.2012.11.004
10. C. De Marco, *et al.*, *ACS applied materials and interfaces* **2** (2010) 2377-2384. doi: 10.1021/am100393e
11. Z. Ding, J. Chen, S. Gao, J. Chang, J. Zhang, and E.T. Kang, *Biomaterials* **25** (2004) 1059-1067.
12. E.S. Gadelmawla, M.M. Koura, T.M.A. Maksoud, I.M. Elewa, H.H. Soliman, *Journal of Materials Processing Technology* **123** (2002) 133-145. doi:10.1016/S0924-0136(02)00060-2
13. C. Gottschalk, and H. Frey, *Macromolecules* **39** (2006) 1719-1723. doi: 10.1021/ma0513259
14. E. Hendrick, and M. Frey, *Journal of Engineered Fabrics and Fibers (JEFF)* **9** (2014) 153-164. Open Access <http://www.jeffjournal.org/papers/Volume9/V9I2-19%20M.%20Frey.pdf>
15. B. Hergelová, A. Zahoranová, D. Kováčik, M. Stupavská, and M. Černák, *Open Chemistry* **13** (2015). doi:10.1515/chem-2015-0067.
16. ImageJ 2015. National Institutes of Health, USA. <http://imagej.nih.gov/ij/>
17. Ingeo 2003, Biopolymer 2003D *Technical Data Sheet NW2003D_051915V1* http://www.natureworkslc.com/~media/Technical_Resources/Technical_Data_Sheets/TechnicalData_Sheet_2003D_FFP-FSW_.pdf
18. ISO25178 Geometrical product specifications (GPS)-Surface texture: Areal-Part 2: *Terms, definitions and surface texture parameters* http://www.iso.org/iso/iso_catalogue/catalogue_tc/catalogue_detail.htm?csnumber=42785
19. H.J. Jeon, and M.N. Kim, *International Biodeterioration and Biodegradation* **85** (2013) 289-293.
20. M.T. Khorasani, H. Mirzadeh, and S. Irani, *Radiation Physics and Chemistry* **77** (2008) 280-287.
21. G.H. Koo, and J. Jang, *Fibers and Polymers* **9** (2008) 674-678. doi: 10.1007/s12221-008-
22. M. Lück, K.F. Pistel, Y.X. Li, T. Blunk, R.H. Müller, and T. Kissel, *Journal of controlled release* **55** (1998) 107-120.
23. A. Marmur, *Langmuir* **19** (2003) 8343-8348. doi: 10.1021/la0344682
24. R. Morent, *et al.*, *The European Physical Journal Applied Physics* **43** (2008) 289-294. doi: 10.1051/epjap:2008076
25. M. Okada, *Progress in polymer science* **27** (2002) 87-133. doi:10.1016/S0079-6700(01)00039-9
26. R.M. Rasal, *Surface and bulk modification of poly (lactic acid) dissertation* Clemson University (2009).
27. R.M. Rasal and D.E. Hirt, *Macromolecular bioscience* **9** (2009) 989-996. doi: 10.1002/mabi.200800374
28. R.M. Rasal and D.E. Hirt, *Macromolecular Materials and Engineering* **295** (2010) 204-209. doi: 10.1002/mame.200900195
29. S.S. Ray, and M. Okamoto, *Macromolecular Rapid Communications* **24** (2003) 815-840. doi: 10.1002/marc.200300008
30. C.H. Schugens, *et al.*, *Journal of Biomedical Materials Research Part A* **29** (1995) 1349-1362. doi : 10.1002/jbm.820291106
31. A.F. Stalder, G. Kulik, D., Sage, L. Barbieri, and P. Hoffmann, *Colloids and surfaces A: physicochemical and engineering aspects* **286** (2006) 92-103. doi:10.1016/j.colsurfa.2006.03.008
32. Tsuji Hideto, *Advanced drug delivery reviews* **107** (2016) 97-135.
33. A.S. Van Dyke, D. Collard, M.M. Derby, and A.R. Betz, *Applied Physics Letters* **107** (2015) 141602. doi: 10.1063/1.4932050
34. R.N. Wenzel, *The Journal of Physical Chemistry* **53** (1949) 1466-1467. doi: 10.1021/j150474a015
35. G. Yu, J. Ji, H. Zhu., and J. Shen, *Journal of Biomedical Materials Research Part B: Applied Biomaterials* **76** (2006) 64-75.
36. Z. Zhang, and S.S. Feng., *Biomaterials* **27** (2006) 4025-4033. doi:10.1016/j.biomaterials.2006.03.006
37. K.J. Zhu, L. Xiangzhou, and Y. Shilin, *Journal of Applied Polymer Science* **39** (1990) 1-9. doi: 10.1002/app.1990.070390101